Atomic Distance Estimates from Disulfides and High-Affinity Metal-Binding Sites in a K^+ Channel Pore

Howard S. Krovetz, Hendrika M. A. VanDongen, and Antonius M. J. VanDongen
Department of Pharmacology, Duke University Medical Center, Durham, North Carolina 27710 USA

ABSTRACT The pore of potassium channels is lined by four identical, highly conserved hairpin loops, symmetrically arranged around a central permeation pathway. Introduction of cysteines into the external mouth of the drk1 K channel pore resulted in the formation of disulfide bonds that were incompatible with channel function. Breaking these bonds restored function and resulted in a high-affinity Cd^{2+}-binding site, indicating coordinated ligation by multiple sulfhydryls. Dimeric constructs showed that these disulfide bonds formed between subunits. These results impose narrow constraints on intersubunit atomic distances in the pore that strongly support a radial pore model. The data also suggest an important functional role for the outer mouth of the pore in gating or permeation.

INTRODUCTION

Ion channels are large integral membrane proteins that consist of subunits or domains symmetrically arranged around an aqueous, ion-conducting pore. Voltage-dependent K^+ channels assemble from identical subunits, each containing six putative transmembrane segments, S1-S6 (Jan and Jan, 1989). The pore of an ion channel is comprised of a narrow region defining ion selectivity and permeation, which is flanked by widening internal and external vestibules. The external vestibule and the outer mouth of the channel were initially localized using an isoform of charybdotoxin, a pore-blocking scorpion toxin that displays a high-affinity for the *Shaker* K^+ channel (Mackinnon and Miller, 1989; Mackinnon et al., 1990). Amino acid residues identified in these studies flank a highly conserved region that was subsequently shown to contribute to the narrow part of the pore (Hartmann et al., 1991; Yellen et al., 1991; Yool and Schwarz, 1991). Because this stretch of amino acids, the P-region, was flanked on both sides by external residues, it was proposed that it forms a re-entrant loop structure (Fig. 1 *A*). Subsequent mutagenesis studies have identified amino acids in the P-region important for selectivity and permeation (Heginbotham et al., 1992; Kirsch et al., 1992; Taglialatela et al., 1993; Heginbotham et al., 1994).

In a theoretical model originally proposed for the structure of the P-region, both the descending (P1) and ascending (P2) limbs of the hairpin loop contributed equally to the pore lining by forming an antiparallel, eight-stranded β-barrel (Bogusz and Busath, 1992; Durell and Guy, 1992). Recently, structural information on the pore has been obtained using several approaches. The outer area of the narrow portion of the pore was estimated to be ~8 Å wide, based on experiments using the pore blocker tetraethylammonium (Heginbotham and Mackinnon, 1992). Surface accessibility of residues in the pore was determined by probing cysteine-substituted mutants with sulfhydryl specific reagents (Kurz et al., 1995; Lu and Miller, 1995; Pascual et al., 1995). Recently, sites of interaction between scorpion toxins with known structures and the *Shaker* K^+ channel have been determined, which have resulted in a toxin footprint or molecular interaction surface (Hidalgo and Mackinnon, 1995; Aiyar et al., 1996; Gross and Mackinnon, 1996; Naranjo and Miller, 1996; Ranganathan et al., 1996). Results from these structural studies have failed to support a β-strand structure for the P-region, suggesting instead a nonperiodic structure. In the *Shaker* K channel, the external mouth of the pore has been shown to undergo conformational changes during C-type inactivation that alter side-chain accessibility (Yellen et al., 1994) or cause a local constriction (Liu et al., 1996). These structural inferences as well as results from mutagenesis studies in Na^+ and Ca^{2+} channels have yielded new theoretical models for the pore of ion channels (Lipkind and Fozzard, 1994; Guy and Durell, 1995; Lipkind et al., 1995).

Another approach that could yield estimates of interatomic distances involves the introduction of cysteines resulting in 1) coordinated metal-binding sites, or 2) the formation of disulfide bonds (Careaga and Falke, 1992). This approach has been previously used for the *Shaker* channel where C-type inactivation greatly enhanced both metal affinity and the formation of a disulfide bond (Yellen et al., 1994; Liu et al., 1996). Zinc and cadmium are transition-IIB metals that display high affinity for cysteine thiolates (Christianson, 1991). Several proteins, including many transcription factors and enzymes, use this property to form high-affinity metal-binding sites in which the divalent ion plays a structural or catalytic role. A common metal-binding motif is the zinc-finger domain in which an extremely high affinity for transition-IIB metals is obtained by coordinated ligation in a well-defined tetrahedral geometry

Received for publication 20 June 1996 and in final form 2 October 1996.
Address reprint requests to Dr. Antonius M.J. VanDongen, Department of Pharmacology, Duke University Medical Center, P.O. Box 3813, Durham, NC 27710. Tel.: 919-681-4862; Fax: 919-684-8922; E-mail: vando005@mc.duke.edu.

0006-3495/97/01/117/10 $2.00

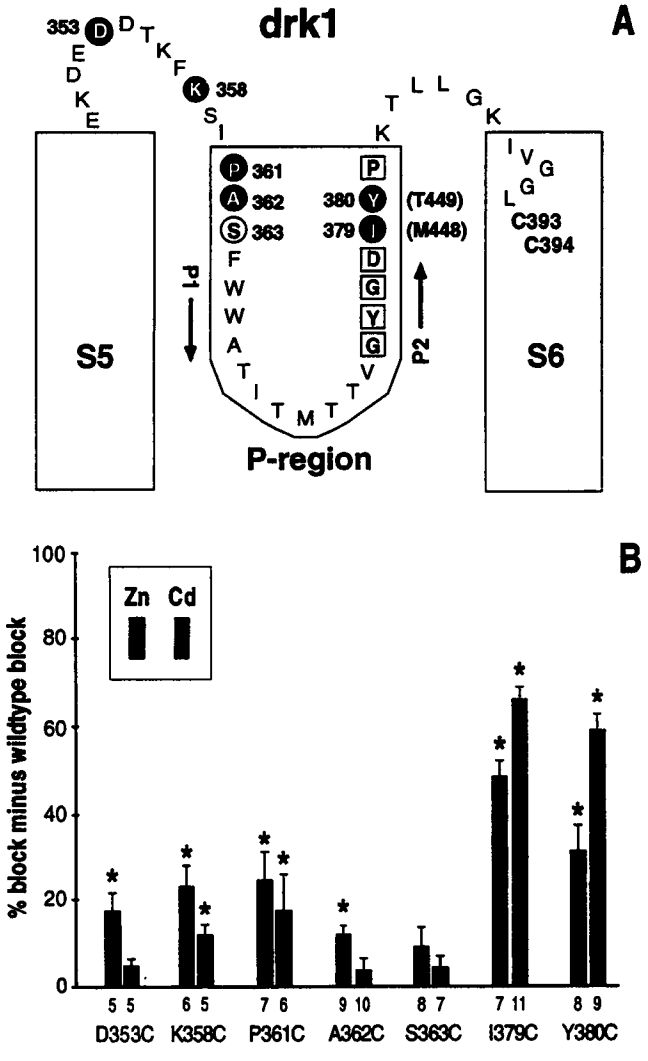

FIGURE 1 Enhanced metal binding in single cysteine-substitution mutants. (*A*) Twelve residues in the outer mouth and P-region of drk1 were individually mutated to cysteine. Mutations that were lethal or expressed poorly are enclosed by a square; functional mutations are enclosed by a circle. Residues for which cysteine substitution resulted in an enhanced inhibition by cadmium (Cd^{2+}) or zinc (Zn^{2+}) are shown on a black background. (*B*) Divalent cation profiles for the functional mutants. Currents were measured in the absence and presence of 1 mM Cd^{2+} and Zn^{2+} in the high-K solution. Both Cd^{2+} and Zn^{2+} produced rapid and reversible inhibition of outward currents elicited by test depolarizations to 0 mV. Means and standard errors were calculated for each group and a one-way ANOVA was performed, followed by Fisher's paired least significant difference test. The bars represent the mean differences in cation block between the mutant and the wt group. Error bars represent standard errors. Asterisks indicate statistical significance ($p < 0.05$). The number of oocytes tested is given below each bar.

(Christianson, 1991; Vallee and Auld, 1993). Both disulfide bonds and metals bound to their high-affinity sites constrain backbone translation and rotation of side chains, which could interfere with protein function. Additionally, bound divalent ions produce an electrostatic field, possibly affecting nearby charges.

To obtain further structural information on the pore region we have introduced novel disulfide bonds and high-affinity metal-binding sites into the pore of the drk1 K^+ channel by cysteine substitution mutagenesis. These novel properties put narrow constraints on several atomic distances in the entry to the narrow part of the pore. These distances are consistent with the previously proposed radial geometry for this region, wherein the carboxy-terminal residues of the P-region are closer to the central axis of the pore than the amino-terminal residues (Guy and Seetharamulu, 1986). Residues in the external mouth seem to play a critical role in gating and/or permeation that has not been previously recognized.

MATERIALS AND METHODS

Molecular biology

Mutagenesis was performed using polymerase chain reaction and drk1 in the pBluescript plasmid vector. Oligonucleotides were designed using the OLIGO software (National Biosciences, Inc., Plymouth, MN). Mutagenesis of small restriction fragments was performed by the "Megaprimer" technique (Sarkar and Sommer, 1990). Mutated fragments were sequenced using a 7-deaza-dGTP DNA Sequencing Kit (Amersham, Cleveland, OH). Plasmid DNA was linearized using the Not I restriction enzyme. Sense RNA was transcribed using T7 RNA polymerase. RNA was capped using m7G(5′)ppp(5′)G.

Construction of dimers

Dimers were constructed using a *SphI* restriction site located at nucleotide 1700 in the C-terminus of drk1 (amino acid 560). A novel drk1 construct was made by introducing an *SphI* restriction site 20 nucleotides upstream of the start codon, which maintains the reading frame at nucleotide 1700 and introduces four glycine residues. Digestion of this vector with *SphI* yielded a 1.7-kb fragment encoding amino acids 1–560. This fragment was ligated into a drk1 construct linearized with *SphI* to produce the tandem dimer. Ion selectivity and activation properties of the wild-type/wild-type (wt/wt) dimer were indistinguishable from the wild-type (wt) subunit expressed as a homotetramer.

Electrophysiology

Oocyte preparation and cRNA injection were done as previously described (VanDongen et al., 1990; Wood et al., 1995). Defolliculated oocytes were placed in a recording chamber perfused with one of the following solutions (concentrations in mM): Divalent-free solution: 100 LiCl 10 HEPES; High-K solution: 85 NaCl, 20 KCl, 1 $MgCl_2$, 10 HEPES; Low-K solution: 100 NaCl, 2 KCl, 1 $MgCl_2$, 10 HEPES. The pH was adjusted to 7.40 using NaOH for all solutions. K^+ currents were recorded using a commercial two-electrode voltage clamp amplifier (Warner Instruments, Hamden, CT). Oocytes were impaled with two electrodes filled with 3 M KCl. The resistances of the current and voltage electrodes were 0.3–1.5 and 1.0–4.0 Mohm, respectively. Voltage pulse protocols and data acquisition were managed by PClamp hardware and software (Axon Instruments, Foster City, CA). Linear leak and capacitive currents were corrected using a P/4 protocol. Inhibition by Cd^{2+} or Zn^{2+} was evaluated using step depolarizations (0 or +40 mV) from a holding potential of −80 mV. Oocytes were perfused continuously with one of the above solutions to which $CdCl_2$ or $ZnCl_2$ was added to obtain the desired concentration.

Statistical analysis

Statistical significance was evaluated using a one-way analysis of variance, followed by Fisher's paired least significant difference test.

RESULTS AND DISCUSSION

Enhanced metal binding of single cysteine substitution mutants

To assess surface accessibility of residues in the P-regions (Fig. 1 *A*), 12 amino acids in the outer mouth and the conserved GYGD sequence of the drk1 K^+ channel were individually mutated to cysteine. As reported previously (Kurz et al., 1995), mutations in the GYGD region were not tolerated, whereas P381C gave rise to very small currents (<1% of drk1 wt) that were not further characterized. Of the remaining seven functional mutants, six were found to be sensitive to divalent cations (Fig. 1 *B*). Two mutations were introduced in the outer vestibule at positions that affect charybdotoxin affinity in *Shaker*. These mutations, D353C and K358C, displayed an enhanced sensitivity to Zn^{2+}. In the descending limb of the hairpin loop, P361C and A362C exhibited increased sensitivity to inhibition by Zn^{2+}. In the ascending limb, I379C and Y380C showed a more substantial increase in divalent sensitivity. These mutants in the C-terminal part of the P-region were more sensitive to Cd^{2+} than Zn^{2+}, whereas the opposite was true for the N-terminal positions. In all sensitive mutants, the divalent block developed rapidly and was fully reversible, indicating that the sulfhydryls were readily accessible to divalent ions from the aqueous pore. These results confirm and expand earlier findings in drk1 (Kurz et al., 1995) with the exception that we found A362 to be exposed. Because the homologous residue in *Shaker*, D431, is exposed as well, the accessibility profiles for *Shaker* and drk1 appear to be conserved (Lu and Miller, 1995; Gross and Mackinnon, 1996).

Coordination of Cd^{2+} binding in I379C, but not Y380C

Mutants I379C and Y380C in the ascending limb of the loop were found to be most sensitive to inhibition by 1 mM of Zn^{2+} or Cd^{2+}. Inhibition due to 1 mM of Cd^{2+} was more complete than 1 mM of Zn^{2+}. These mutants were studied further to investigate the molecular basis for their increased Cd^{2+} sensitivity. Full-dose-reponse curves showed that saturating concentrations of Cd^{2+} completely inhibited K^+ currents in both mutants (Fig. 2 and Table 1). This indicates that the presence of a cysteine at position 379 or 380 resulted in the appearance of one or more Cd^{2+}-binding sites, the occupancy of which is incompatible with K^+ channel function. The Cd^{2+} concentration necessary to block half of the K^+ current (IC_{50}) was 10-fold lower for I379C (26 μM) than Y380C (256 μM). Because K^+ channels assemble from four identical subunits, single cysteine substitutions result in the introduction of four cysteines in the pore. These could form four independent binding sites with each sulfhydryl ligating a Cd^{2+} ion. Alternatively, cysteines in neighboring subunits could bind Cd^{2+} in a coordinated fashion, resulting in an increased affinity. To distinguish between these alternatives, tandem dimers were

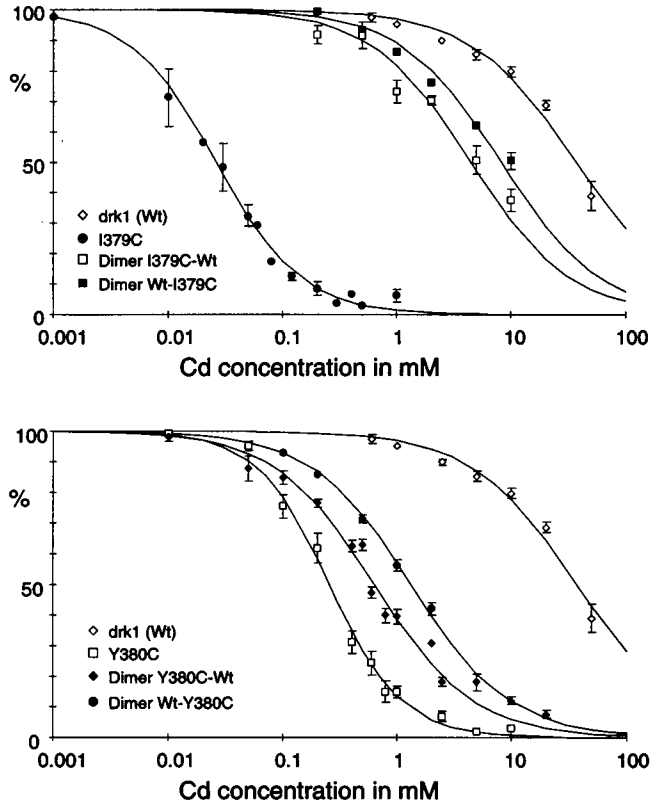

FIGURE 2 Coordinated Cd^{2+} binding in I379C, but not Y380C. The concentration-dependence of Cd^{2+} inhibition was determined for drk1, I379C, and Y380C, as well as dimeric tandem constructs that combine a drk1 wt subunit with a mutant subunit in both orientations. Cd^{2+} dose-inhibition curves were determined using the divalent-free LiCl solution. Each point represents a minimum of five separate recordings. Currents were elicited by 300-ms step depolarizations to +40 mV from a holding potential of −80 mV. The inhibition by Cd^{2+} was rapid and reversible. Dose-inhibition curves were fitted with the Hill equation: $I(c) = 1/(1 + (c/IC_{50})^N)$, where I is the fraction of K^+ current left after Cd^{2+} inhibition, c is the Cd^{2+} concentration used, N is the Hill coefficient, and IC_{50} is the Cd^{2+} concentration required to inhibit 50% of the K^+ current. The curve fit results are summarized in Table 1. (*A*) Cd^{2+} dose-inhibition curves for drk1, I379C, and the dimers I379C-wt and wt-I379C. An equation for four independent binding sites (Heginbotham and Mackinnon, 1992) predicts an IC_{50} of 52 μM for the dimers from the IC_{50}'s of the parents drk1 (37 mM) and I379C (26 μM): $K_{dimer} = 2K_{wt}K_{mutant}/(K_{wt} + K_{mutant})$, where K stands for IC_{50}. It is assumed that a single bound metal ion is capable of inhibiting the observed current. The actual IC_{50}s for the dimers (4.5 mM and 8.2 mM) are shifted much further to the right, indicating a lack of independence. (*B*) Cd^{2+} dose-inhibition curves for drk1, Y380C, and the dimers Y380C-wt and wt-Y380C. The equation for four independent sites predicts an IC_{50} of 0.51 mM for the dimers, which is close to the actual IC_{50}s of 0.64 mM and 1.3 mM.

constructed containing both a mutant and a wt subunit. These dimers are expected to form channels in which the pore contains only two cysteines that are located across from each other. Channels formed from dimers containing a single I379C subunit were ~100-fold less sensitive to Cd^{2+} than homotetrameric I379C channels (Fig. 2 *A* and Table 1). In contrast, the Cd^{2+} IC_{50} for channels formed from dimers containing a single Y380C subunit was close to the predicted value for four independent binding sites (Fig. 2 *B* and

TABLE 1 Cd^{2+} IC_{50}s and Hill coefficients in divalent-free solution

Construct	IC_{50}	Hill
Wildtype	37 mM	1.0
I379C	26 μM	1.2
Y380C	256 μM	1.4
Dimer I379C-Wt	4.5 mM	1.0
Dimer Wt-I379C	8.2 mM	1.0
Dimer Y380C-Wt	0.64 mM	1.0
Dimer Wt-Y380C	1.3 mM	1.0
I379C + Y380C	20 nM	1.0

Currents were elicited by a 300-ms step depolarization to +40 mV from a holding potential of −80 mV. Percent inhibition was calculated from the inhibition of the steady-state outward current by Cd^{2+}. All experiments were done in the divalent-free solution. Oocytes expressing I379C+Y380C were treated with 1 mM DTT for 12–36 h prior to testing.

Table 1). These results suggest coordination of Cd^{2+} by cysteines in neighboring subunits at position I379 and conversely, a lack of coordination at the Y380 position.

The orientation of the dimer had a small effect on Cd^{2+} affinity. This can be explained if a small fraction (<10%) of the channels assemble using only the front half of the dimers. Experiments in which dimers were expressed that contained a lethal subunit (F364S) and a wt subunit indicated that <5% of the channels assemble using only the wt portion of the dimer (data not shown). Thus, a large fraction of the observed whole cell current results from properly incorporated dimers.

Introduction of a novel disulfide bond and a high-affinity Cd^{2+}-binding site

In an attempt to construct a much higher affinity Cd^{2+}-binding site, a double mutation combining I379C and Y380C was constructed. This I379C+Y380C double mutant was found to express very poorly, giving rise to minute K^+ currents. However, treatment of the oocytes with the reducing agent dithiothreitol (DTT) fully restored K^+ channel function, suggesting the presence of one or more novel disulfide bonds (Fig. 3 *A*). Whereas complete recovery of function took several hours to develop, DTT could be shown to increase the current in minutes (Fig. 3 *B*). This acute effect suggests that the channels containing the disulfide bonds are already present in the plasma membrane, but function poorly. The fact that disulfide bonds spontaneously formed in the I379C+Y380C double mutant, but not in the two parents I379C and Y380C suggests that disulfide bonds form between cysteines at positions 379 and 380. However, the S6 transmembrane segment contains two cysteine residues at positions 393 and 394 (Fig. 1 *A*). To investigate a possible contribution of the two S6 cysteines, the I379C+Y380C double mutation was made with either or both S6 cysteines mutated to serine. All of these constructs required DTT to restore function (Fig. 3 *C*). Because the presence of cysteines at positions 379 and 380 is necessary and sufficient for formation of a disulfide bond, it is likely that a disulfide bond forms between these positions. Interestingly, two of these mutants (I379C+Y380C+C393S and I379C+Y380C+C393S+C394S) displayed an absolute requirement for external K^+ ions. All of the constructs were therefore measured in the presence of 2 mM external KCl.

After reduction by DTT, the I379C+Y380C double mutant was found to have a very high affinity for cadmium. Fig. 4 *A* shows a representative block of this channel by 100 nM Cd^{2+} in a divalent-free solution. Extensive washing (20 min) did not appreciably recover the current until EDTA was added. Due to the length of the protocol used to assess this high-affinity block, the recovery of the currents was incomplete. Therefore, current levels after recovery were used to calculate the degree of block to avoid overestimating the inhibition of currents. The I379C+Y380C double mutant was >1000-fold more sensitive to Cd^{2+} than either of the parent constructs, indicating coordinated ligation of Cd^{2+} by sulfhydryls at positions 379 and 380 (Fig. 4 *B* and Table 1).

Again, this high-affinity (nM) binding site for Cd^{2+} did not require the presence of cysteines in S6 (Table 2). Mutating both S6 cysteines to serines did produce a small (two- to sixfold) reduction in the IC_{50} for Cd^{2+} in all constructs tested. They can do so directly by making a (relatively weak) contribution to the Cd^{2+}-binding site or indirectly by slightly altering the pore conformation through a propagative effect. The sixfold effect of removing both S6 cysteines on Cd affinity of I379C+Y380C seen in the different constructs pales in comparison to the 3000- to 10,000-fold reduction of affinity seen upon removal of a single cysteine from either position 379 or 380. To test this further, Cd^{2+} affinities were determined for constructs containing a single cysteine, as well as all possible combinations of two cysteines at positions 379, 380, 393, and 394. From these measurements, coupling coefficients (Ωs) were calculated for each cysteine pair (Hidalgo and MacKinnon, 1995), which are shown in Table 3. Clearly, the cysteines at positions 379 and 380 make a distinct, highly cooperative contribution to the Cd-binding site, whereas the S6 cysteines do not.

Disulfide bonds form between subunits

To determine whether the disulfide bonds between the cysteines at position 379 and 380 are formed within the same subunit or between neighboring subunits, a dimer was constructed that only supported intersubunit disulfide bonds. The front half of this dimer consisted of I379C, whereas the back half was Y380C. This I379C-Y380C dimeric construct was readily modifiable by reducing and oxidizing reagents (Fig. 5 *A*), whereas the I379C-wt, wt-Y380C, and wt/wt dimers were not affected (Table 4). The fact that redox modulation of the I379C-Y380C dimer depended critically on the simultaneous presence of both pore cysteines strongly supports the hypothesis that an intersubunit disulfide bond exists between positions 379 and 380.

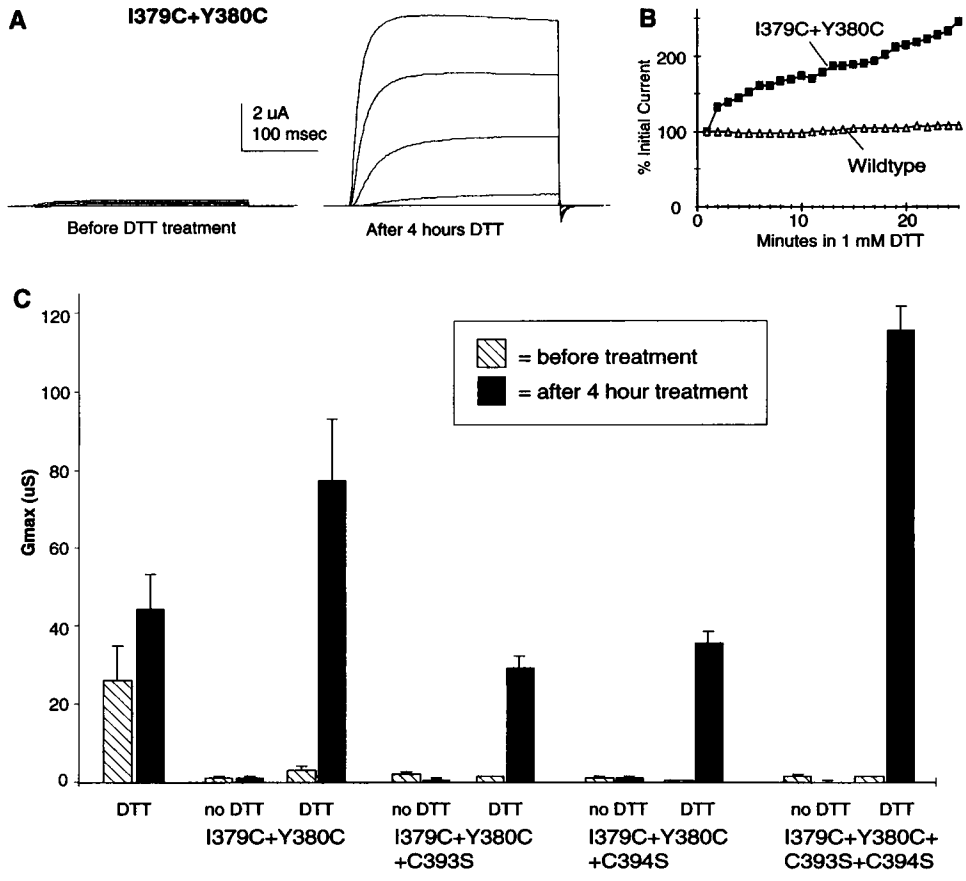

FIGURE 3 Disulfide bonds form in the I379C+Y380C double mutant. (*A*) Families of currents of the I379C+Y380C double mutant 36 h after cRNA injection, before and after a 4-h treatment with 1 mM DTT. Currents were elicited by 300-ms test pulses between −40 and +40 mV in 20-mV increments, from a holding potential of −80 mV. Oocytes were continuously perfused with low-K solution. (*B*) Time course of DTT modification for wt drk1 and the I379C+Y380C double mutant. Currents were elicited by a 300-ms step depolarization to +40 mV from a holding potential of −80 mV. The interpulse interval was 60 s. Currents at the end of the test pulse were measured, normalized using the initial current value and plotted against time. (*C*) Two cysteines in S6 (C393 and C394) are not involved in the DTT requirement of the I379C+Y380C mutant. Families of currents were recorded from oocytes expressing the various constructs, before and after a 4 h period in which the oocytes were either treated with 1 mM DTT or left untreated. Average whole cell conductances are plotted for each group of oocytes. Pulse protocol and solutions were the same as in *A*. All experiments were started 36 h after cRNA injection. Differences in whole cell K conductances between constructs may have resulted from differences in expression levels between batches of oocytes or differences in folding efficiency.

Oxidation with 0.1% H_2O_2 decreased the whole cell current and reached a steady-state inhibition of 50% within 60 s. A subsequent treatment with DTT restored the current to a value greater than 100%, suggesting that the channels were partially oxidized at the start of the experiment. Indeed, DTT was found to increase the K^+ current in untreated oocytes (Fig. 5 *B*, *inset*). This implies that disulfide bonds form in some of the channels in the absence of oxidizing reagents. The fact that complete oxidation of the I379C-Y380C dimer only reduces the current by 50% suggests that channels containing intersubunit disulfide bonds are still able to function. If this were the case, current reduction would result from an alteration of channel function, not from an increase in the number of nonfunctional channels.

If the cysteines I379C and Y380C were involved in an intersubunit disulfide bond, they would not be available as ligands for Cd^{2+}. Therefore, the affinity for Cd^{2+} of the I379C-Y380C dimer was measured under reducing and oxidizing conditions (Fig. 6). In the reduced state, the Cd^{2+} affinity of the I379C-Y380C dimer was much higher than any parent construct, again implying coordinated ligation by both sulfhydryls at the interface between subunits. Oxidation was found to shift the Cd^{2+} affinity >400-fold. The loss of high-affinity Cd^{2+} binding after oxidation suggests that these cysteines in the pore become involved in intersubunit disulfide bonds. Furthermore, these oxidized channels are still functional, because a shift in affinity would not be observed if the presence of disulfide bonds removed the channel from the functional pool.

Structural inferences

The objective of this study was to derive structural information by introducing disulfide bonds and high-affinity

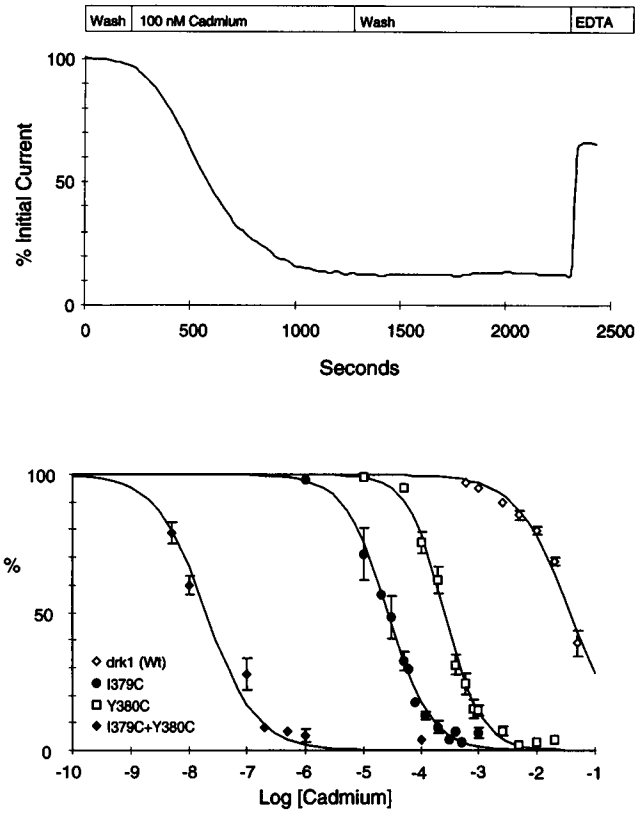

FIGURE 4 The reduced form of I379C+Y380C contains a high-affinity Cd^{2+}-binding site. (*A*) Time course of the inhibition of I379C+Y380C by 100 nM Cd^{2+} in divalent-free solution. Outward currents were elicited by 300-ms depolarizing pulses to +40 mV. Oocytes were pretreated with DTT. Extensive washing with divalent-free solution did not reverse the inhibition. Cd^{2+} block was quickly relieved upon the addition of 0.25 mM EDTA. (*B*) Cd^{2+} dose-inhibition curves for drk1, I379C, Y380C, and I379C+Y380C. Curves were fitted with the Hill equation (see Table 1). Pulse protocol is the same as in Fig. 2. All experiments were performed in the divalent-free LiCl solution to which $CdCl_2$ was added.

metal-binding sites in the external mouth of a K channel pore using cysteine substitution mutagenesis. In part, our evidence depends on manipulating the redox state of the channel by using H_2O_2 and DTT. In addition to promoting the formation of disulfide bonds, H_2O_2 also can lead to the oxidation of the cysteine sulfhydryl group to sulfenic acid, whereas DTT can reverse both reactions. Several arguments suggest that the observed current inhibition results from formation of disulfide bonds rather than alternative oxidative products. First, the double mutant I379C+Y380C requires reduction by DTT to function, whereas both parents I379C and Y380C do not. Second, the I379C-Y380C dimer can be modulated by redox reagents, whereas the I379C-wt and the wt-Y380C dimers can not. The fact that the simultaneous presence of cysteines at both positions 379 and 380 results in the emergence of a new property indicates a strong cooperativity between cysteines at these positions, consistent with disulfide formation. In contrast, oxidation of free thiolates to sulfenic acid would be expected to affect individual cysteines and display additivity.

The strongest evidence for the presence of intersubunit disulfide bonds comes from the redox modulation of Cd^{2+} affinity in the I379C-Y380C dimer construct. The loss of high-affinity binding upon oxidation suggests that one or both disulfides are formed in this dimer. We have no evidence that all four putative disulfide bonds are formed in the I379C+Y380C double mutant. However, the nearly complete loss of function of the oxidized form of the I379C+Y380C double mutant suggests that more disulfides are formed in this construct than in the I379C-Y380C dimer, where function is only partially lost upon oxidation.

The disulfide bonds and high-affinity metal-binding sites characterized here can be used to derive a structural model of this region of the pore. Introduction of one or more cysteines at positions 379 and 380 does not appear to affect K channel function, as long as the cysteines remain reduced. The structural inferences that are drawn here are based on cysteines that are involved either in disulfide bridges or binding metal ions. Therefore, an important question is whether disulfide bond formation or divalent cation binding traps the protein in a rare conformation. Large amplitude internal motions are not uncommon in proteins and can result in disulfide formation between distant cysteines (Careaga and Falke, 1992). The rate at which disulfide formation occurs depends on 1) the distance between the two cysteines and 2) the relative thermal mobility of the protein backbone (Careaga and Falke, 1992). Other important factors include the temperature, the concentration and characteristics of the redox reagents used, and the pH. The I379C-Y380C dimer is readily oxidized by 0.1% H_2O_2 with a time constant of ~10 s (Fig. 5), suggesting that either these residues are in close proximity or are involved in large amplitude movements. Without additional information on backbone mobility, it is difficult to derive an accurate estimate of the translational movement required for disulfide bond formation.

The absence of function of the nonreduced I379C+Y380C double mutant indicates that the protein is trapped in an unfavorable conformation. However, the I379C-Y380C dimer does function upon oxidation, suggesting that the formation of up to two disulfide bonds does not alter the protein conformation drastically. Additionally, the very high affinity of the I379C+Y380C double mutant for Cd^{2+} is an argument against a scenario wherein the coordination of a Cd^{2+} ion forces the sulfhydryls into an energetically unfavorable conformation.

Atomic distances and pore geometry

Taken together, the results presented here render a detailed model of the outer mouth of the drk1 K^+ channel pore at the level of I379 and Y380. The disulfide bonds and high-affinity metal-binding sites introduced into the pore impose narrow constraints on atomic distances and geometry in this part of the protein (Fig. 7). All the interatomic distances for two cysteine residues involved in a disulfide bond are

TABLE 2 Cd^{2+} IC_{50}s and Hill coefficient in low-K solution

Construct	−DTT		+DTT	
	IC_{50}	Hill	IC_{50}	Hill
Wildtype	36 mM	1.0	30 mM	1.0
C393S+C394S	101 mM	1.0	52 mM	1.1
I379C	130 μM	1.6	120 μM	1.3
I379C+C393S+C394S	550 μM	1.3	500 μM	1.4
Y380C	450 μM	2.0	450 μM	2.0
Y380C+C393S+C394S	1.4 mM	2.0	1.3 mM	2.0
I379C+Y380C	N.D.	N.D.	44 nM	1.5
I379C+Y380C+C393S+C394S	N.D.	N.D.	252 nM	1.7

The protocol used was the same as in Table 1, except that all experiments were done in the low-K solution. Cd^{2+} inhibition curves were obtained both with and without DTT pretreatment (1 mM for 12–36 h). DTT had only minor effects on the IC_{50} and Hill coefficient.

TABLE 3 Coupling coefficients (Ω) for pairs of cysteines at positions 379, 380, 393, and 394

Position	379	380	393
394	3.3	1.7	1.5
393	2.5	2.2	
380	49.2		

Cadmium dose-response curves were obtained for constructs containing 0, 1, or any combination of two cysteines at positions 379, 380, 393, and 394. IC_{50}s for Cd^{2+} were estimated by fitting the Hill equation (see legend of Fig. 2) to the dose-response data. In addition to the constructs reported in Table 2, the following IC_{50} values were obtained: C393S 48 mM; C394S 48 mM; I379C+C393S 140 μM; I379C+C394S 1.2 mM; Y380C+C393S 690 μM; Y380C+C394S 2.6 mM. These values were used to calculate coupling coefficients (Ω) in a thermodynamic mutant cycle analysis (Hidalgo and MacKinnon, 1995): $\Omega = (X_{c1} * X_{c2})/(X_0 * X_{c1+c2})$, where X represents IC_{50} values for mutants with no cysteines (X_0), one cysteine (X_{c1} and X_{c2}) and both cysteines (X_{c1+c2}). Interaction-strength is measured by the degree of deviation from unity.

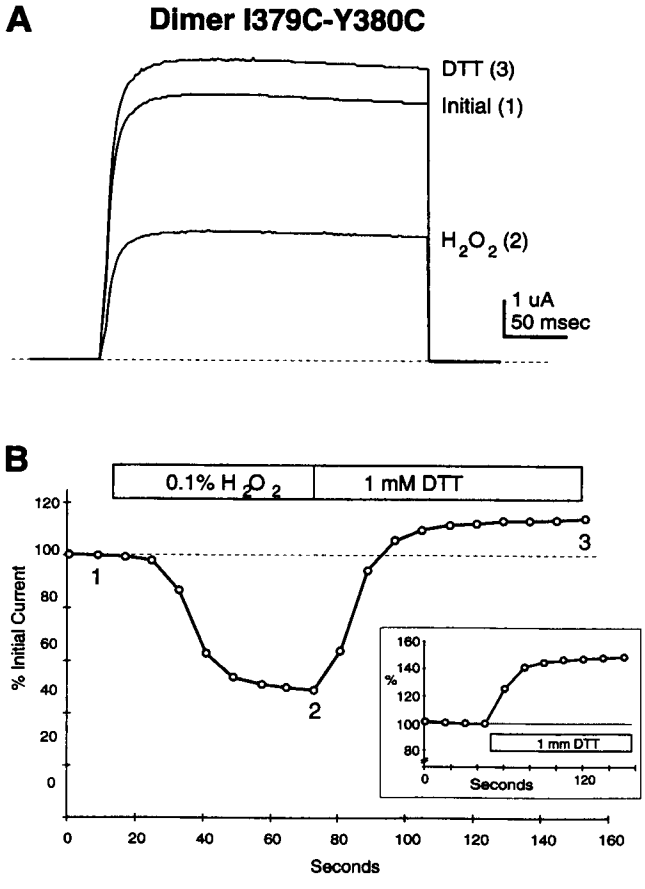

FIGURE 5 Redox modulation of the I379C-Y380C dimer. (*A*) Effect of oxidation (0.1% H_2O_2) and reduction (1 mM DTT) on the I379C-Y380C dimer. Currents were elicited by a 300-ms step depolarization to +40 mV from a holding potential of −80 mV. Oocytes were continuously perfused with the low-K solution. (*B*) Time course of oxidation and reduction of the I379C-Y380C dimeric construct. The *inset* illustrates that even without prior exposure to an oxidizing reagent the current is increased upon treatment of the oocyte with 1 mM DTT.

known (Fig. 7 *A*). Due to several rotational degrees of freedom, the distance between the α carbons (C_αs) of the cysteines involved are not precisely defined, but rather constrained to a narrow range. Together with the 3.8-Å distance between two consecutive C_αs in a protein, both intra- and intersubunit C_α distances can now be estimated for positions 379 and 380 (Fig. 7 *A*). Breaking the disulfides after reduction would allow the structure to relax, thereby moving C_α380 and C_α379′ further apart. However, the high-affinity Cd^{2+}-binding site that appears after reduction implies coordinated ligation by at least two sulfhydryls. The two most likely candidates are the same cysteines that form the intersubunit disulfide bond upon oxidation. From this, a new distance estimate can be derived, suggesting that the distance between intersubunit C_αs only increases by ~1 Å (Fig. 7 *B*). Coordination of Cd^{2+} by I379C, but not Y380C (Fig. 2), resulted in a further refinement of the model such that the I379 residues were located closer to the central axis of the pore than the Y380 residues (Fig. 7 *B*). The diameter of the outer mouth at positions 379 and 380 estimated from the model shown in Fig. 7 is consistent with a study that used TEA to estimate an 8-Å pore diameter at position 449 in *Shaker* (Heginbotham and Mackinnon, 1992), which is homologous with Y380 in drk1. In the "iris" model recently proposed to explain the accessibility profile of the cyclic nucleotide-gated channels (Sun et al., 1996), positions homologous to I379 and Y380 would have to be located near the central axis of the pore making up the turn of the loop.

The distance and geometry constraints illustrated in Fig. 7, *A* and *B*, severely limit the possible arrangements of the

TABLE 4 Redox modulation of dimer constructs

Construct	Mean	SEM	*N*
Wt-Wt	97.6%	0.6%	7
I379C-Wt	96.9%	1.3%	9
Wt-Y380C	99.2%	0.6%	7
I379C-Y380C	47.5%	6.2%	7

To evaluate redox sensitivity, dimer constructs were treated with H_2O_2 and DTT, while recording K currents, as shown in Fig. 5. Currents were elicited every 15 s by a 300-ms step depolarization to +40 mV from a holding potential of −80 mV. Oocytes were continuously perfused with the low-K solution. After establishing a baseline for 75 s, oocytes were treated with 0.1% H_2O_2 for 150 s, followed by 1 mM DTT for 75 s. Steady-state outward K currents were plotted as a function of time (Fig. 5 *b*). Redox sensitivity was calculated as the current at the end of the H_2O_2 treatment, divided by the current following reduction by DTT.

P-region hairpin loops around the pore (Fig. 7 *C*). The originally proposed eight-stranded barrel does not support an intersubunit disulfide between I379C and Y380C, because only one of the two residues could face into the pore. The problem cannot be resolved by assuming that the two limbs of the hairpin (P1 and P2) are not fully hydrogen bonded. The possibility of forming an intersubunit disulfide bond between two consecutive residues in P2 is inconsistent with any model in which P1 and P2 are interspersed with both limbs making an equivalent contribution to the pore lining. Theoretical models in which P2 is closer to the central axis than P1 have been proposed for voltage-gated K^+, Na^+, and Ca^{2+} channels (Guy and Seetharamulu, 1986; Lipkind and Fozzard, 1994; Guy and Durell, 1995; Lipkind et al., 1995). Our data strongly support such radial models for the outer mouth of the pore, in which the descending

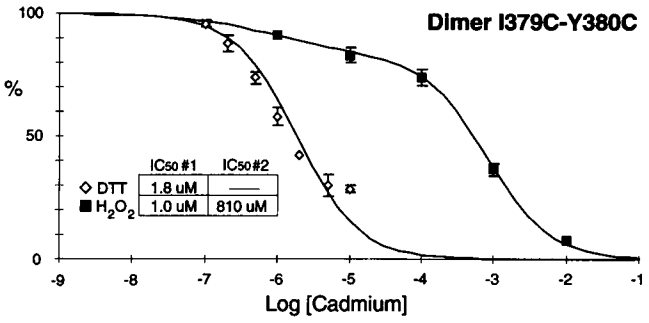

FIGURE 6 Redox modulation of the cadmium affinity of the I379C-Y380C dimer. Cadmium dose-inhibition curves for the I379C-Y380C dimer. The oocytes were treated with either 1 mM DTT or 0.1% H_2O_2 until a steady baseline was obtained (see Fig. 5). Cadmium was then applied and inhibition of currents was measured. The curve for the DTT-treated oocytes was fitted with the standard Hill equation (Fig. 2). The oxidized form of the I379C-Y380C dimer exhibited a low-affinity site as well as a higher affinity site. The curve for H_2O_2-treated oocytes was therefore fitted with an equation for two binding sites: % Current = $F/(1 + [Cd]/IC50_1) + (1 - F)/(1 + [Cd]/IC50_2)$, where F is the fraction of high-affinity binding sites. The IC_{50} of the higher affinity site corresponds well to the Cd^{2+} affinity of the DTT-treated channels, suggesting that 17% (F) of the channels were not oxidized. Currents were elicited by a 300-ms step depolarization to +40 mV from a holding potential of −80 mV. Oocytes were continuously perfused with low-K solution.

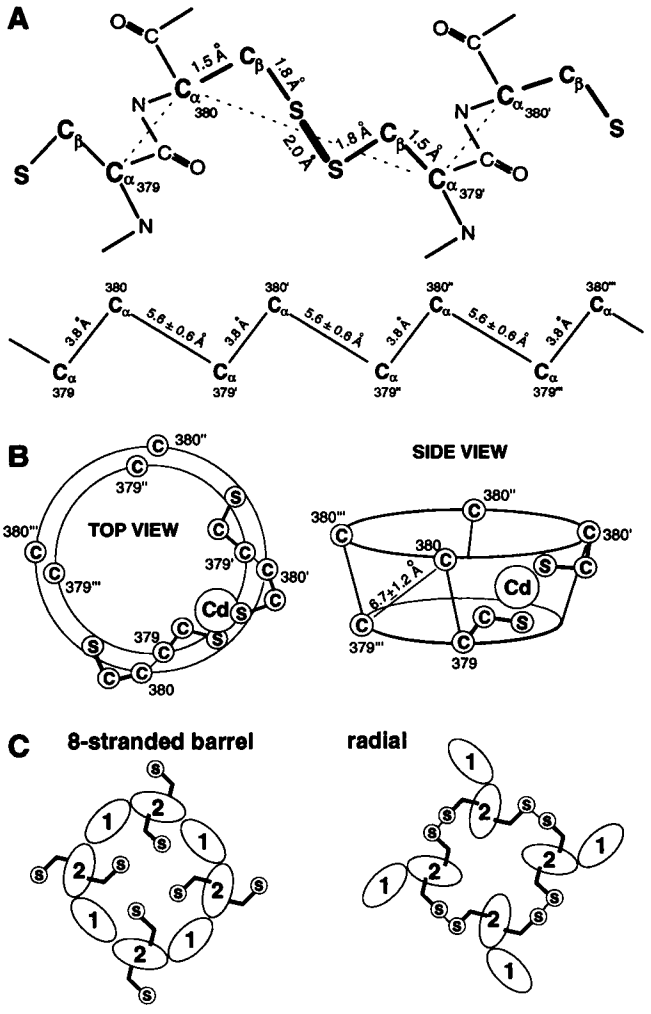

FIGURE 7 Structural consequences of disulfide bonds and high-affinity metal-binding sites. (*A*) Interatomic distances for a disulfide bond formed between a cysteine at position 380 in one subunit and a cysteine at position 379′ in a neighboring subunit. A fully extended two-dimensional representation is shown, in which the C_α380-C_α379′ distance is overestimated. Actual C_α-C_α distances were determined from 23 disulfide bonds in 8 proteins with a known crystal structure. Distances ranged from 4.4 to 6.7 Å with a mean and standard deviation of 5.6 ± 0.6 Å. This information together with the 3.8-Å distance between consecutive C_αs in the protein backbone constrains the structure of a bracelet formed by four pairs of C_αs. (*B*) Top and side views of the C379 and C380′ residues coordinating a Cd^{2+} ion. High-affinity Cd^{2+} and Zn^{2+}-binding sites in proteins share a tetrahedral coordination geometry. The distance between the C_αs at position 379 and 380 was estimated from the crystal structures of zinc-finger proteins, containing either Zn^{2+} or Cd^{2+}. The distance between 18 pairs of cysteine C_αs ranged from 5.3 to 9.3 Å, with a mean and standard deviation of 6.7 ± 1.2 Å. To explain the difference in Cd^{2+} coordination displayed by the single cysteine substitution mutants I379C and Y380C, C_α380 is placed further away from the central pore axis than C_α379. (*C*) A fourfold, symmetrical, eight-stranded, antiparallel barrel model precludes formation of intersubunit disulfide bonds between two consecutive residues (379 and 380). In this model the pore is lined by both descending and ascending limbs of the P-region hairpin loop, indicated here by ovals labeled 1 and 2, respectively. The long axis of the ovals indicates the direction of hydrogen bonding. Rotating the P-region loops such that the descending limb (P1) moves away from the central axis while maintaining fourfold symmetry results in a radial pore model that supports formation of disulfide bonds.

limb P1 is placed at a distance further away from the central axis (Fig. 7 *C*).

Functional inferences

The data presented here also suggest a critical role in permeation or gating for the external mouth of the drk1 K channel. The apparent small reduction in pore diameter associated with oxidation of the four disulfide bonds would seem unlikely to occlude the pore sufficiently to disallow permeation of K ions. Alternatively, it is proposed that movement of the side chains at position 379 or 380 may be required either for opening the channel or for ion permeation. Binding of Cd^{2+} ions would also restrict side-chain movement. In addition, bound Cd^{2+} would interfere with K^+ ion permeation by electrostatic repulsion. The importance of this latter effect is illustrated by the fact that Cd^{2+} almost completely inhibits the K^+ current in the I379C-Y380C dimer, whereas formation of up to two disulfides only results in a partial inhibition.

Movement of the protein backbone at residue 449 in the *Shaker* K^+ channel, a position equivalent with Y380, has been suggested to be associated with C-type inactivation. Substitution of cysteine for threonine at this position (T449C) resulted in a Zn^{2+}-binding site wherein affinity dramatically increased after C-type inactivation (Yellen et al., 1994). A mutation in *Shaker* (M448C) that introduces a cysteine at a position equivalent with I379 results in the spontaneous formation of a disulfide bond (Gross and Mackinnon, 1996; Liu et al., 1996). Reformation of this disulfide bond was shown to be enhanced by C-type inactivation. Inactivation in drk1 is much slower and does not depend upon the presence of the C-terminus (VanDongen et al., 1990). In our experiments, inactivation of the channel by prolonged depolarization did not enhance the rate of disulfide formation (data not shown).

Formation of disulfide bridges between adjacent subunits can impede channel function by a reduction of the single channel conductance, a decrease in open probability, or a combination of these two effects. Presence of a disulfide bond will interfere with the dynamic behavior of the cysteine residues involved by 1) reducing the rotational degrees of freedom of the side chains, and 2) restricting how far their backbones can move apart. One or both of these dynamic aspects seems to be essential for channel function at positions 379 and 380. The data obtained for the I379C-Y380C dimer suggest that restriction of movement in two of the four subunit interfaces is not lethal, whereas presence of all four intersubunit disulfides in the double mutant I379C+Y380C results in loss of function. Therefore, the dynamics of subunit interfaces may play a critical role in channel function.

We would like to thank Jane Richardson, Homme Hellinga, Pat Casey, and Richard Whorton for helpful discussions, and Tony Lacerda for suggesting LiCl as a divalent-free solution.

This work was supported by grant NS31557 from the National Institute of Neurological Disorders and Stroke to A.M.J.V.D.

REFERENCES

Aiyar, J., J. M. Withka, J. P. Rizzi, D. H. Singleton, G. C. Andrews, W. Lin, J. Boyd, D. C. Hanson, M. Simon, B. Dethlefs, C.-l. Lee, J. E. Hall, A. G. Gutman, and K. G. Chandy. 1996. Topology of the pore-region of a K channel revealed by the NMR-derived structures of scorpion toxins. *Neuron.* 15:1169–1181.

Bogusz, S., and D. Busath. 1992. Is a beta-barrel model of the K channel energetically feasible? *Biophys. J.* 62:23–25.

Careaga, C. L., and J. J. Falke. 1992. Thermal motions of surface alpha-helices in the D-galactose chemosensory receptor. *J. Mol. Biol.* 226: 1219–1235.

Christianson, D. W. 1991. Structural biology of zinc. *Adv. Protein Chem.* 42:281–355.

Durell, S. R., and H. R. Guy. 1992. Atomic scale structure and functional models of voltage-gated potassium channels. *Biophys. J.* 62:238–250.

Gross, A., and R. Mackinnon. 1996. Agitoxin footprinting the *Shaker* potassium channel pore. *Neuron.* 16:399–406.

Guy, H. R., and S. R. Durell. 1995. Structural models of Na^+, Ca^{2+}, and K^+ channels. *Soc. Gen. Physiol. Ser.* 50:1–16.

Guy, H. R., and P. Seetharamulu. 1986. Molecular model of the action potential sodium channel. *Proc. Natl. Acad. Sci. USA.* 83:508–512.

Hartmann, H. A., G. E. Kirsch, J. A. Drewe, M. Taglialatela, R. H. Joho, and A. M. Brown. 1991. Exchange of conduction pathways between two related potassium channels. *Science.* 251:942–944.

Heginbotham, L., T. Abramson, and R. Mackinnon. 1992. A functional connection between pores of distantly related ion channels as revealed by mutant K+ channels. *Science.* 258:1152–1155.

Heginbotham, L., Z. Lu, T. Abramson, and R. Mackinnon. 1994. Mutations in the K channel signature sequence. *Biophys. J.* 66:1061–1067.

Heginbotham, L., and R. Mackinnon. 1992. The aromatic binding site for tetraethylammonium ion on potassium channels. *Neuron.* 8:483–491.

Hidalgo, P., and R. Mackinnon. 1995. Revealing the architecture of a K+ channel pore through mutant cycles with a peptide inhibitor. *Science.* 268:307–310.

Jan, L. Y., and Y. N. Jan. 1989. Voltage-sensitive ion channels. *Cell.* 56:13–25.

Kirsch, G. E., J. A. Drewe, H. A. Hartmann, M. Taglialatela, M. De Biasi, A. M. Brown, and R. H. Joho. 1992. Differences between the deep pores of K+ channels determined by an interacting pair of nonpolar amino acids. *Neuron.* 8:499–505.

Kurz, L. L., R. D. Zuhlke, H. J. Zhang, and R. H. Joho. 1995. Side-chain accessibilities in the pore of a K^+ channel probed by sulfhydryl-specific reagents after cysteine-scanning mutagenesis. *Biophys. J.* 68:900–905.

Lipkind, G. M., and H. A. Fozzard. 1994. A structural model of the tetrodotoxin and saxitoxin binding site of the Na^+ channel. *Biophys. J.* 66:1–13.

Lipkind, G. M., D. A. Hanck, and H. A. Fozzard. 1995. A structural motif for the voltage-gated potassium channel pore. *Proc. Natl. Acad. Sci. USA.* 92:9215–9219.

Liu, Y., M. E. Jurman, and G. Yellen. 1996. Dynamic rearrangement of the outer mouth of a K channel during gating. *Neuron.* 16:859–867.

Lu, Q., and C. Miller. 1995. Silver as a probe of pore-forming residues in a potassium channel. *Science.* 268:304–307.

Mackinnon, R., L. Heginbotham, and T. Abramson. 1990. Mapping the receptor site for charybdotoxin, a pore-blocking potassium channel inhibitor. *Neuron.* 5:767–771.

Mackinnon, R., and C. Miller. 1989. Mutant potassium channels with altered binding of charybdotoxin, a pore-blocking peptide inhibitor. *Science.* 245:1382–1385.

Naranjo, D., and C. Miller. 1996. A strongly interacting pair of residues on the contact surface of charybdotoxin and a *Shaker* K^+ channel. *Neuron.* 16:123–130.

Pascual, J. M., C. C. Shieh, G. E. Kirsch, and A. M. Brown. 1995. K^+ pore structure revealed by reporter cysteines at inner and outer surfaces. *Neuron.* 14:1055–1063.

Ranganathan, R., J. H. Lewis, and R. Mackinnon. 1996. Spatial localization of the K^+ channel selectivity filter by mutant cycle-based structure analysis. *Neuron.* 16:131–139.

Sarkar, G., and S. S. Sommer. 1990. The "megaprimer" method of site-directed mutagenesis. *BioTechniques.* 8:404–407.

Sun, Z. P., M. H. Akabas, E. H. Goulding, A. Karlin, and S. A. Siegelbaum. 1996. Exposure of residues in the cyclic nucleotide-gated channel pore: P region structure and function in gating. *Neuron.* 16:141–149.

Taglialatela, M., J. A. Drewe, G. E. Kirsch, M. De Biasi, H. A. Hartmann, and A. M. Brown. 1993. Regulation of K^+/Rb^+ selectivity and internal TEA blockade by mutations at a single site in K^+ pores. *Pflügers Arch.* 423:104–112.

Vallee, B. L., and D. S. Auld. 1993. Zinc: biological functions and coordination motifs. *Acc. Chem. Res.* 26:543–551.

VanDongen, A. M. J., G. C. Frech, J. A. Drewe, R. H. Joho, and A. M. Brown. 1990. Alteration and restoration of K+ channel function by deletions at the N- and C-termini. .*Neuron* 5:433–443.

Wood, M. W., H. M. A. VanDongen, and A. M. J. VanDongen. 1995. Structural conservation of ion conduction pathways in K channels and glutamate receptors. *Proc. Natl. Acad. Sci. USA* 92:4882–4886.

Yellen, G., M. E. Jurman, T. Abramson, and R. Mackinnon. 1991. Mutations affecting internal TEA blockade identify the probable pore-forming region of a K channel. *Science* 251:939–942.

Yellen, G., D. Sodickson, T.-Y. Chen, and M. E. Jurman. 1994. An engineered cysteine in the external mouth of a K+ channel allows inactivation to be modulated by metal binding. *Biophys. J.* 66:1068–1075.

Yool, A. J., and T. L. Schwarz. 1991. Alteration of ionic selectivity of a K channel by mutation of the H5 region. *Nature.* 349:700–704.